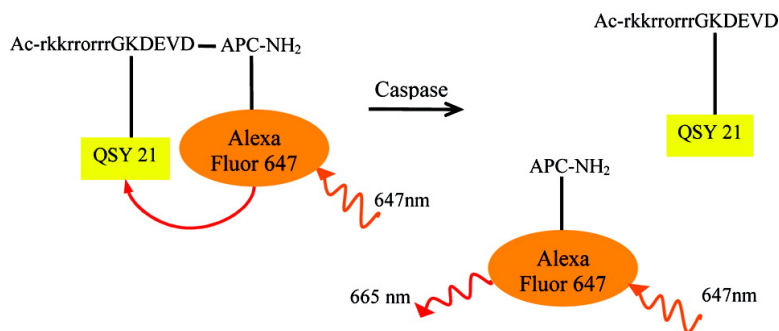


Synthesis and Characterization of a Small, Membrane-Permeant, Caspase-Activatable Far-Red Fluorescent Peptide for Imaging Apoptosis

Kristin Bullok, and David Piwnica-Worms

J. Med. Chem., **2005**, 48 (17), 5404-5407 • DOI: 10.1021/jm050008p • Publication Date (Web): 04 August 2005

Downloaded from <http://pubs.acs.org> on March 28, 2009



More About This Article

Additional resources and features associated with this article are available within the HTML version:

- Supporting Information
- Links to the 7 articles that cite this article, as of the time of this article download
- Access to high resolution figures
- Links to articles and content related to this article
- Copyright permission to reproduce figures and/or text from this article

[View the Full Text HTML](#)

Letters

Synthesis and Characterization of a Small, Membrane-Permeant, Caspase-Activatable Far-Red Fluorescent Peptide for Imaging Apoptosis

Kristin Bullok and David Piwnica-Worms*

Molecular Imaging Center, Mallinckrodt Institute of Radiology, and Department of Molecular Biology and Pharmacology, Washington University, St. Louis, Missouri 63110

Received January 5, 2005

Abstract: To image apoptosis *in vivo* with a small, membrane-permeant probe, TcapQ₆₄₇ was synthesized comprising a Tat-peptide-based permeation peptide sequence, an effector caspase recognition sequence, DEVD, and a flanking optically activatable pair comprising a far-red quencher, QSY 21, and a fluorophore, Alexa Fluor 647. Under baseline conditions, high quenching efficiencies were observed resulting in low background fluorescence. Upon exposure to executioner caspases, TcapQ₆₄₇ was specifically cleaved, thereby releasing the fluorophore from the quencher and enabling imaging of apoptosis.

Apoptosis, or programmed cell death, is fundamental to normal development and deregulated apoptosis contributes to various disease states including neurodegenerative disorders, cardiovascular disease, and cancer.^{1,2} Noninvasive clinical diagnosis of apoptosis to guide therapeutic choices and monitor treatment provides the impetus to develop apoptosis-specific molecular imaging probes. However, current apoptotic imaging probes are not completely apoptotic specific^{3,4} or have large molecular weights⁵ that can limit tissue diffusion.^{6,7} Thus, improved injectable apoptotic probes are desired for clinical diagnosis. At the apex of apoptosis, the caspase family of proteases, specifically executioner caspases 3, 6, and 7, are activated,^{8,9} thereby inducing cell death. Thus, we designed and synthesized a small, membrane-permeant caspase activatable imaging probe, TcapQ₆₄₇ (Figure 1), to specifically image cellular commitment to apoptosis.

TcapQ₆₄₇ is a small peptidomimetic comprising an all D-amino acid Tat-peptide-based permeation peptide sequence, rkkrrrrr, to afford facile and concentrative cell penetration,^{10,11} and an L-amino acid effector caspase recognition sequence, DEVD, that is flanked by the far-red quencher, QSY 21, and the fluorophore, Alexa Fluor 647. Placement of the permeation peptide sequence at the N-terminus of the caspase recognition sequence was determined as the optimal design from preliminary studies showing enhanced kinetics over C-terminal placement (data not shown). Utilization of a cleavable, quenched far-red fluorescence strategy afforded low fluorescent background, specificity, signal amplification, and opportunities for higher detection sensitivity in deep

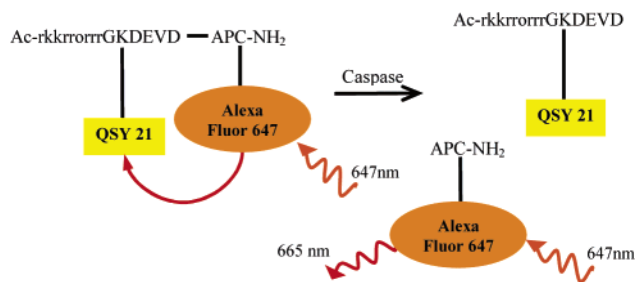


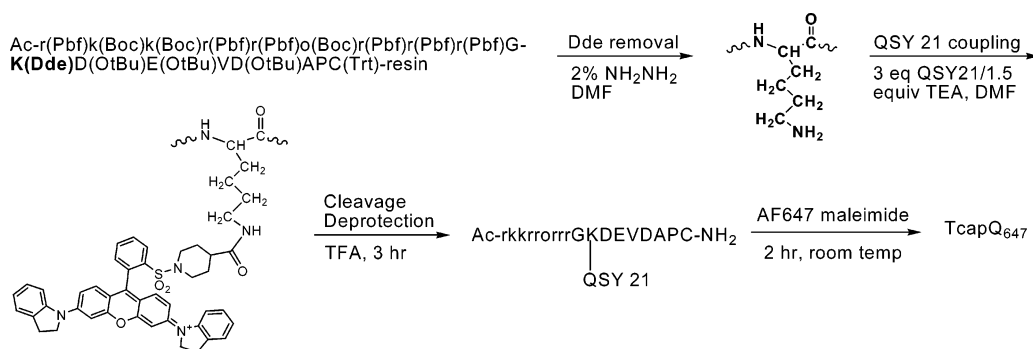
Figure 1. Model of TcapQ₆₄₇ cleavage by executioner caspases.

tissue. Thiol conjugation of Alexa Fluor 647 at the C-terminus should enable executioner caspase-mediated cleavage and intracellular accumulation of the fluorophore fragment. Additionally, the modest molecular weight of TcapQ₆₄₇ should improve tissue diffusion compared to larger probes. This communication will focus on the initial characterization and validation of the utility of TcapQ₆₄₇ in imaging apoptosis *in cellulo*.

The peptide backbone of TcapQ₆₄₇ was synthesized by solid-phase peptide synthesis using standard Fmoc chemistry. Subsequently, while the protected amino acids of the peptide remained on resin, the Dde protecting group on the lysine adjacent to the recognition sequence was selectively removed using 2% hydrazine in DMF (Scheme 1). Following selective lysine deprotection, the resin was dried and QSY 21 succinimide in anhydrous DMF was transferred under argon into a sealed vial containing the peptide on resin. Coupling of QSY 21 to the primary amine of the lysine was allowed to proceed overnight. Following extensive washes with DMF and acetonitrile, the resin was dried before simultaneously deprotecting and cleaving the peptide from resin using TFA. Finally, Alexa Fluor 647 maleimide was thiol-conjugated to the C-terminal cysteine of the peptide to obtain TcapQ₆₄₇. A control, noncleavable quenched peptide, dTcapQ₆₄₇, composed of all D-amino acids was synthesized in a similar manner. In addition, an unquenched control peptide, T₆₄₇, composed only of the Tat-peptide-based permeation sequence with a C-terminal cysteine conjugated to Alexa Fluor 647 was synthesized.

TcapQ₆₄₇ was purified by RP-HPLC¹² and characterized through electrospray mass spectrometry (*m/z*: 3927.0; calc 3927.2), absorption spectrometry, and fluorometry. Absorption spectrometry of TcapQ₆₄₇ revealed an absorption maximum at 605 nm, which is blue-shifted from the absorption maximum of T₆₄₇ at 650 nm. The blue-shifted absorption spectrum observed with TcapQ₆₄₇ is indicative of a strong Coulombic interaction between the QSY 21 and Alexa Fluor 647 chromophores.¹³ The extinction coefficient at 605 nm was determined to be 211 500 M⁻¹ cm⁻¹. Finally, the fluorescence quenching efficiency of TcapQ₆₄₇ was determined by fluorometry following a 60 min incubation at 37 °C in milliQ water, in DMEM media with 10% heat-

* Corresponding author. Phone: 314-362-9356. Fax: 314-362-0152. E-mail: piwnica-wormsd@mir.wustl.edu.

Scheme 1. Synthesis of TcapQ₆₄₇

inactivated fetal bovine serum, and in 100% heat-inactivated fetal bovine serum. Under all conditions, high fluorescence quenching of TcapQ₆₄₇ was observed using this single quencher-fluorophore pair (Figure 2). Calculated quenching efficiencies were between 92% and 99%.

To determine the ability of executioner caspases to recognize and cleave TcapQ₆₄₇, an extensive endpoint assay with recombinant caspase 3 (CalBiochem; 52 h with addition of fresh enzyme at 24 h; 50 U) at 37 °C was performed.¹⁴ The formation of product was monitored using HPLC, which indicated enhancement of a peak ($t_R = 18.5$ min) with a time that corresponded to the positive control peptide, APC(Alexa Fluor 647)-amide, indicating sequence-specific TcapQ₆₄₇ cleavage by recombinant caspase 3. This peak was not observed upon incubation of dTcapQ₆₄₇ with recombinant caspase 3. In addition, the 18.5 min peak obtained as a result of cleavage was collected and characterized through electrospray mass spectrometry. The analysis confirmed it to be the expected C-terminal enzymatic product (m/z : 1269.1; calc 1268.0).

TcapQ₆₄₇ cleavage by executioner caspases (caspase 7 and 3) was then analyzed by fluorometry, and rate of cleavage was compared with an initiator caspase (caspase 9). Enzyme kinetic studies were performed by incubating recombinant caspases (CalBiochem) in buffer containing TcapQ₆₄₇ at 37 °C, and enhancement in fluorescence was monitored over time. Fluorometry revealed significant increases in fluorescence over background for caspase 7 and 3, confirming that TcapQ₆₄₇ is recognized and cleaved by the executioner caspases, but not by the initiator caspase. Rates of cleavage within the linear regime were determined to be 50 FU/min over background (caspase 7; Figure 3), 1 FU/min over background

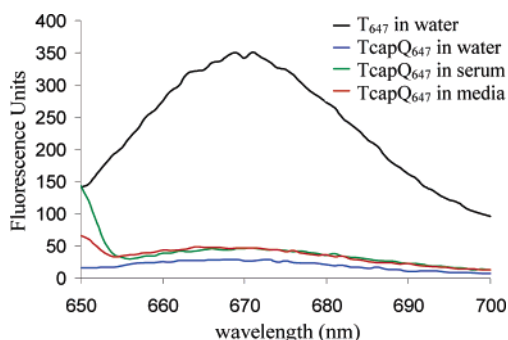


Figure 2. Fluorescence emission spectra of quenched TcapQ₆₄₇ (2 μ M) and unquenched control, T₆₄₇ (2 μ M), in various solutions following a 60 min incubation at 37 °C.

(caspase 3), and 0.3 FU/min over background (caspase 9) indicating that caspases 7 and 3 cleave TcapQ₆₄₇ at a 170-fold and 3.5-fold higher rate than caspase 9, respectively. TcapQ₆₄₇ cleavage was further characterized by caspase inhibition assays. The reversible caspase inhibitor, DEVD-CHO, prevented cleavage of TcapQ₆₄₇ by both recombinant caspase 7 (IC₅₀ = 11 nM) and 3 (IC₅₀ = 1.2 nM) in a concentration-dependent manner.

To demonstrate intracellular delivery, localization, and activation of TcapQ₆₄₇ by native enzymes, apoptosis was induced in KB 3-1 tumor cells by pretreatment for 13 h with 0.2 μ M vinblastine, with or without a caspase inhibitor, or for 13 h with 2 μ M vinblastine before addition of TcapQ₆₄₇ or dTcapQ₆₄₇, respectively. After a 20 min peptide incubation, TcapQ₆₄₇ activation was determined by monitoring fluorescence (>650 nm, far-red) with live-cell confocal microscopy (Figure 4A and 4B). As shown, TcapQ₆₄₇ activation was observed in vinblastine-treated cells but not in caspase-inhibited and vinblastine-treated cells, providing direct evidence for intracellular delivery and caspase-specific activation of the imaging probe. Upon incubation of vinblastine-treated cells with the control all D-amino acid peptide, dTcapQ₆₄₇, no fluorescence was observed (Figure 4C), further indicating that the observed fluorescence in TcapQ₆₄₇-incubated cells is enzyme dependent. In addition, incubation of cells with a general caspase substrate, (L-aspartate)₂-rhodamine 110 (D₂R),¹⁵ resulted in activation and colocalization of D₂R with TcapQ₆₄₇, thus confirming the presence and activation of executioner caspases in apoptotic cells (data not shown).

To quantitatively determine activation of TcapQ₆₄₇ *in cellulo*, flow cytometry analysis on Jurkat cells, treated

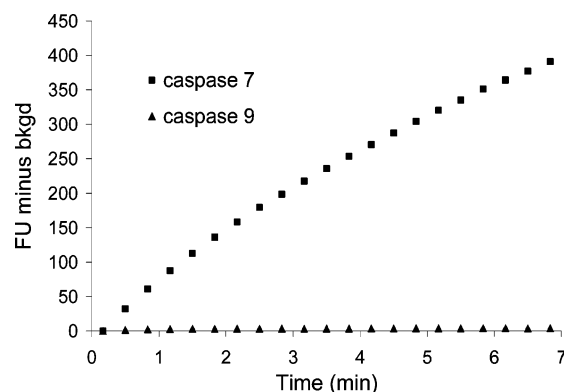


Figure 3. Fluorescence activation of TcapQ₆₄₇ (2 μ M) by recombinant caspase 7 and caspase 9 (5 U each) as measured by fluorometry.

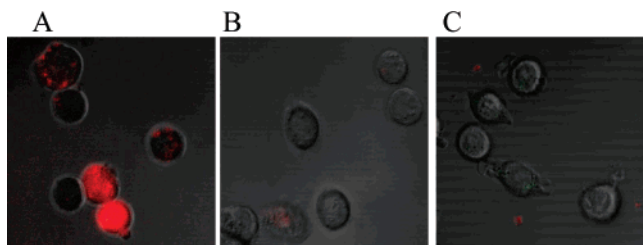


Figure 4. Live-cell fluorescence microscopy (>650 nm) of TcapQ₆₄₇ activation. (A) KB 3-1 cells were pretreated with vinblastine ($0.2 \mu\text{M}$) for 13 h before incubation with TcapQ₆₄₇ ($4 \mu\text{M}$) for 20 min. (B) Identical to panel A, except the pretreatment buffer included the cell permeable caspase inhibitor, D(OMe)QMD(OMe)-FMK ($20 \mu\text{M}$). (C) KB 3-1 cells were pretreated with vinblastine ($2 \mu\text{M}$) for 13 h before incubation with control dTcapQ₆₄₇ ($4 \mu\text{M}$) for 20 min.

or untreated with C₆-ceramide, was carried out (Figure 5). Incubation of ceramide-treated cells for 30–60 min with TcapQ₆₄₇ resulted in detection of 10% early and late stage apoptotic cells. Incubation of untreated cells with TcapQ₆₄₇ resulted in only 3% apoptotic cells. Further, in ceramide-treated cells incubated with the control dTcapQ₆₄₇, only 4% labeling was observed, which was comparable to the untreated cell population. In comparison, utilization of the commercial caspase substrate, D₂R, resulted in 1% labeling in untreated cells and 22% in ceramide-treated cells. These differences were observed following necessary compensation between channels due to cross-talk between the FL1 and FL3 channels. As expected, a larger percent of cells are labeled with D₂R as compared to TcapQ₆₄₇ since D₂R is an indicator for all active caspases¹⁵ while TcapQ₆₄₇ is an indicator for only executioner caspases.

Of note, no toxicity due to TcapQ₆₄₇ was observed over the course of the cell assays. To further characterize the toxicity of TcapQ₆₄₇, *Renilla luciferase*-expressing KB 3-1 cells were seeded in three independent 96-well plates 24 h before addition of increasing TcapQ₆₄₇ concentrations (1 nM – $100 \mu\text{M}$) in complete media. After a 24 h incubation, the peptide solution was removed and buffer containing coelenterazine was added immediately before obtaining images with a cooled CCD camera (IVIS 100). Cell viability was quantified by bioluminescence photon output as described in Supplemental methods and kill curves for each plate were generated. Taking the average of the curves, the LD₅₀ was determined to be $10 \mu\text{M} \pm 2$. These data correlate with visual observations where cells treated with up to $3 \mu\text{M}$ TcapQ₆₄₇ were viable with only small decreases in viability observed above $3 \mu\text{M}$. Cell death was notable at $10 \mu\text{M}$ followed by a dramatic decrease in viability at $30 \mu\text{M}$. Complete cell death was observed at $100 \mu\text{M}$.

In summary, a novel permeation peptide probe, TcapQ₆₄₇, capable of imaging apoptosis was synthesized. High quenching efficiencies utilizing a single quencher-fluorophore pair were observed under various conditions resulting in very low background fluorescence in the absence of activated executioner caspases. Further, TcapQ₆₄₇ was shown to be effectively and specifically cleaved by executioner caspases both *in vitro* and *in cellulo* confirming the utility of TcapQ₆₄₇ as a probe for imaging apoptosis.

The main advantages of the TcapQ₆₄₇ imaging probe over available agents include a far-red fluorescence

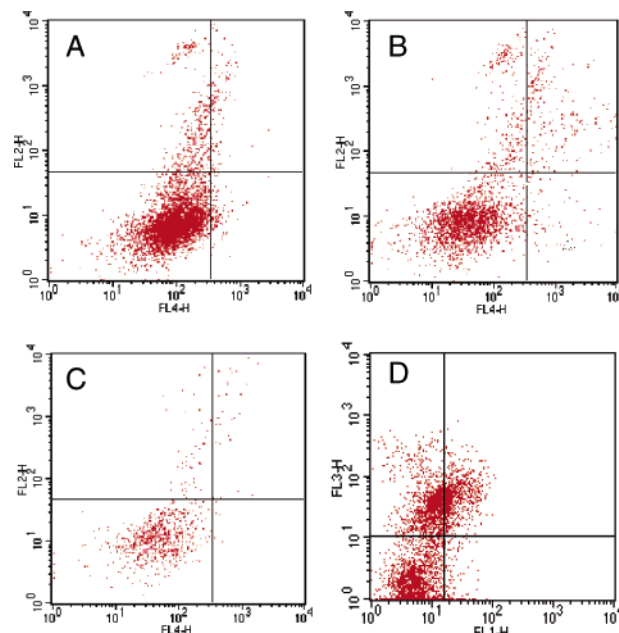


Figure 5. Flow cytometric analysis of Jurkat Cells. (A) Analysis of untreated cells incubated for 30–60 min with TcapQ₆₄₇ ($4 \mu\text{M}$) and propidium iodide (PI; $6 \mu\text{g}/\text{mL}$). (B) Analysis of ceramide-treated ($40 \mu\text{M}$; 4.5 h) cells incubated with TcapQ₆₄₇ and PI as above. (C) Analysis of ceramide-treated cells incubated with dTcapQ₆₄₇ ($4 \mu\text{M}$) and PI ($6 \mu\text{g}/\text{mL}$). (D) Control analysis of ceramide-treated cells incubated with D₂R ($5 \mu\text{M}$) and 7-AAD ($6 \mu\text{g}/\text{mL}$). The apoptotic population was determined from the percent of cells in the upper and lower right quadrants.

emission detectable upon caspase cleavage. Because TcapQ₆₄₇ emits fluorescence above 650 nm, little to no interference from cellular autofluorescence is observed. In addition, flow cytometry analysis of the far-red fluorescence activation of TcapQ₆₄₇ is easily distinguished from propidium iodide, a common nuclear stain used for identifying cells with compromised cell membranes. Apoptotic probes having shorter wavelength properties, including the commercial substrate, D₂R, require practiced compensation of the cytometer to isolate the activated D₂R fluorescence signal from nuclear stains. Finally, imaging probes that emit light above 650 nm have optimal properties for imaging activities *in vivo* as tissue absorption of light is minimal in the far-red and near-infrared spectrum.

A further advantage of the TcapQ₆₄₇ scaffold is the modular design, providing for coupling of alternative quencher-fluorophore pairs with desired optical properties. The TcapQ₆₄₇ scaffold also is amenable to modifications of the cleavage sequence to target different enzymes. Further, these modifications of TcapQ₆₄₇ can be accomplished in a straightforward manner using the methods described above or other standard coupling techniques. In particular, coupling of near-infrared fluorophore-quencher pairs, such as the recently published quencher, NIRQ₈₂₀,¹⁶ to the TcapQ₆₄₇ scaffold could be accomplished to provide increased signal penetration and detection over far-red fluorophores *in vivo*. Applications for TcapQ₆₄₇ would include not only optical imaging of apoptotic cells in culture, but potentially the imaging of apoptotic cells induced by ischemia, inflammation, and neurodegenerative diseases *in vivo*.

We are currently studying the utility of TcapQ₆₄₇ in detecting chemotherapeutic efficacies in vivo.

Acknowledgment. Special thanks to Vijay Sharma, Samuel Achilefu, and Seth Gammon for valuable discussions, the Hope Center for Neurological Diseases at Washington University for confocal microscopy use, and Michelle Rohlfine and Catherine Chang for flow cytometry technical support. This work was supported by NIH grants P50 CA94056 and CA83841.

Supporting Information Available: Detailed synthesis and analysis of TcapQ₆₄₇ and methods for enzyme and cell-based assays. This material is available free of charge via the Internet at <http://pubs.acs.org>.

References

- (1) De Simone, R.; Ajmone-Cat, M.; Minghetti, L. Atypical antiinflammatory activation of microglia induced by apoptotic neurons: possible role of phosphatidylserine-phosphatidylserine receptor interaction. *Mol. Neurobiol.* **2004**, *29*, 197–212.
- (2) Okada, H.; Mak, T. Pathways of apoptotic and nonapoptotic death in tumor cells. *Nat. Rev. Cancer* **2004**, *4*, 592–603.
- (3) Vermes, I.; Haanen, C.; Steffens-Nakken, H.; Reutelingsperger, C. A novel assay for apoptosis: flow cytometric detection of phosphatidylserine expression on early apoptotic cells using fluorescein labelled annexin V. *J Immunol. Meth.* **1995**, *184*, 39–51.
- (4) Brauer, M. In vivo monitoring of apoptosis. *Prog. Neuropsychopharmacol. Biol. Psychiatry* **2003**, *27*, 323–331.
- (5) Zhao, M.; Beauregard, D.; Loizou, L.; Davletov, B.; Brindle, K. Non-invasive detection of apoptosis using magnetic resonance imaging and a targeted contrast agent. *Nat. Med.* **2001**, *7*, 1241–1244.
- (6) Jain, R. The next frontier of molecular medicine: delivery of therapeutics. *Nat. Med.* **1998**, *4*, 665–667.

- (7) Graff, C.; Wittrup, K. Theoretical analysis of antibody targeting of tumor spheroids: importance of dosage for penetration and affinity for retention. *Cancer Res.* **2003**, *63*, 1288–1296.
- (8) Thornberry, N.; Lazebnik, Y. Caspases: enemies within. *Science* **1998**, *281*, 1312–1316.
- (9) Degterev, A.; Boyce, M.; Yuan, J. A decade of caspases. *Oncogene* **2003**, *22*, 8543–8567.
- (10) Bullok, K.; Dyszlewski, M.; Prior, J.; Pica, C.; Sharma, V.; Piwnica-Worms, D. Characterization of novel histidine-tagged Tat-peptide complexes dual labeled with ^{99m}Tc-tricarbonyl and fluorescein for scintigraphy and fluorescence microscopy. *Bioconjugate Chem.* **2002**, *13*, 1226–1237.
- (11) Gammon, S.; Villalobos, V.; Prior, J.; Sharma, V.; Piwnica-Worms, D. Quantitative analysis of permeation peptide complexes labeled with technetium-99m: Chiral and sequence-specific effects on net cell uptake. *Bioconjugate Chem.* **2003**, *14*, 368–376.
- (12) HPLC method: column, Vydak, RP C₁₈, 4.6 mm; A = 0.1% TFA in 5% CH₃CN/H₂O, B = 0.1% TFA in 90% CH₃CN/H₂O, C = 0.1% TFA in CH₃CN; linear gradient, 100% A to 60% A and 40% B over 10 min, then to 54% A and 46% B over 25 min, to 100% B over 7 min followed by a 4 min wash with 100% C before returning to initial conditions.
- (13) Hernando, J.; van der Schaaf, M.; van Dijk, E.; Sauer, M.; Garcia-Parajo, M.; van Hulst, N. Excitonic behavior of rhodamine dimers: a single-molecule study. *J. Phys. Chem. A* **2003**, *107*, 43–52.
- (14) Talanian, R. V.; Quinlan, C.; Trautz, S.; Hackett, M. C.; Mankovich, J. A.; Banach, D.; Ghayur, T.; Brady, K. D.; Wong, W. W. Substrate specificities of caspase family proteases. *J. Biol. Chem.* **1997**, *272*, 9677–9682.
- (15) Hug, H.; Los, M.; Hirt, W.; Debatin, K. Rhodamine 110-linked amino acids and peptides as substrates to measure caspase activity upon apoptosis induction in intact cells. *Biochemistry* **1999**, *38*, 13906–13911.
- (16) Pham, W.; Choi, Y.; Weissleder, R.; Tung, C.-H. Developing a peptide-based near-infrared molecular probe for protease sensing. *Bioconjugate Chem.* **2004**, *15*, 1403–1407.

JM050008P